

Fractional dynamics and recurrence analysis in cancer model

Enrique C. Gabrick^{1*†}, Matheus R. Sales^{1†}, Elaheh Sayari^{1†},
José Trobia^{2†}, Ervin K. Lenzi^{1,3†}, Fernando da S. Borges^{4†},
José D. Szezech Jr.^{1,2†}, Kelly C. Iarosz^{1,5,6†}, Ricardo L. Viana^{6,7†},
Iberê L. Caldas^{7†}, Antonio M. Batista^{1,2,7†}

¹Graduate Program in Science, State University of Ponta Grossa,
84030-900, Ponta Grossa, PR, Brazil.

²Department of Mathematics and Statistics, State University of Ponta
Grossa, 84030-900, Ponta Grossa, PR, Brazil.

³Department of Physics, State University of Ponta Grossa, 84030-900,
Ponta Grossa, PR, Brazil.

⁴Department of Physiology and Pharmacology, State University of New
York Downstate Health Sciences University, 11203, Brooklyn, NY, USA.

⁵University Center UNIFATEB, 84266-010, Telêmaco Borba, PR, Brazil.

⁶Institute of Physics, University of São Paulo, 05508-090, São Paulo, SP,
Brazil.

⁷Department of Physics, Federal University of Paraná, 82590-300,
Curitiba, PR, Brazil.

*Corresponding author(s). E-mail(s): ecgabrick@gmail.com;

†These authors contributed equally to this work.

Abstract

In this work, we analyze the effects of fractional derivatives in the chaotic dynamics of a cancer model. We begin by studying the dynamics of a standard model, *i.e.*, with integer derivatives. We study the dynamical behavior by means of the bifurcation diagram, Lyapunov exponents, and recurrence quantification analysis (RQA), such as the recurrence rate (RR), the determinism (DET), and the recurrence time entropy (RTE). We find a high correlation coefficient between the Lyapunov exponents and RTE. Our simulations suggest that the tumor growth parameter (ρ_1) is associated with a chaotic regime. Our results suggest a high

correlation between the largest Lyapunov exponents and RTE. After understanding the dynamics of the model in the standard formulation, we extend our results by considering fractional operators. We fix the parameters in the chaotic regime and investigate the effects of the fractional order. We demonstrate how fractional dynamics can be properly characterized using RQA measures, which offer the advantage of not requiring knowledge of the fractional Jacobian matrix. We find that the chaotic motion is suppressed as α decreases, and the system becomes periodic for $\alpha \gtrsim 0.9966$. We observe limit cycles for $\alpha \in (0.9966, 0.899)$ and fixed points for $\alpha < 0.899$. The fixed point is determined analytically for the considered parameters. Finally, we discover that these dynamics are separated by an exponential relationship between α and ρ_1 . Also, the transition depends on a supper transient which obeys the same relationship.

Keywords: Cancer model, Fractional Calculus, Recurrence analysis

1 Introduction

Cancer is a set of diseases that arises from the abnormal growth and uncontrolled division of body cells. It can spread to the body's cells, causing many deaths [1]. Each year the American Cancer Society estimates the number of new cancer cases. For 2020 there was an estimated number of 19.3 million new cancer cases and almost 10.0 million deaths from cancer [2]. Only in the United States of America were projected 1,918,030 new cancer cases and 609,360 cancer deaths for 2022 [3]. In this way, cancer is a crucial public health problem worldwide [4] that requires many efforts to understand the mechanism behind the illness and improve the treatment methods [5–7]. There are several methods to study the dynamics of cancer cell proliferation and one of the most successful method is through mathematical models.

Mathematical model is a powerful tool for understanding cancer dynamics [8, 9] and simulate treatment measures, such as effects of drug resistance [10, 11], immunotherapy [12], chemotherapy [13, 14], radiotherapy [15], biochemotherapy [16] and predict fluctuations associated with the growth rate of cancer cells [17]. A fundamental question that arises is how to understand the dynamics among healthy cells, the immune system and the tumor cells. In light of this question, several models have been proposed and studied [18–24].

Dehingia *et al.* [25] studied the effect of time delay in tumor-immune interaction and stimulation process. They obtained conditions for the existence of equilibrium points and Hopf bifurcation. Also, they derived conditions for periodic solutions. Díaz-Marín *et al.* [26] proposed a model to describe cell population dynamics in a tumor with periodic radiation as treatment. As global attractors, they found almost periodic solutions or the vanishing equilibrium. López *et al.* [27] formulated a model for tumor growth in the presence of cytotoxic chemotherapeutic agents. Their model allows an investigation of the Norton-Simon hypothesis in the context of dose-dense chemotherapy. In another work, López *et al.* [28] validated a model by means of experimental results. In this model, they considered tumor growth, including tumor-healthy cell

interactions, immune response, and chemotherapy. Most of these models deal with three or more dimensional systems, where chaotic behavior is a possibility [29].

A three-dimensional cancer model with chaotic dynamics was proposed by Itik and Banks [30]. In their model, they considered the interactions of tumor cells with healthy host cells and immune systems. Through the calculation of Lyapunov exponents, they showed the existence of chaotic attractors for some parameters. Letellier *et al.* [31], made a topological and observability analysis of this model. They also investigated the equilibrium points and the bifurcation diagrams. Khajanchi *et al.* [32] studied a similar model with time delay. They analyzed the existence and stability of biologically feasible points and the emergence of Hopf bifurcations. Chaos in the 3-cell cancer model was also studied by Abernethy and Gooding [33], Gallas *et al.* [34], Khajanchi [35] and others [36–39].

Although the literature about the model proposed by Itik and Banks [30] is extensive, the works are restricted to integer-order differential equations. However, this formulation does not incorporate non-local effects. To do that, it is necessary to consider fractional differential equations [40]. In general, non-local operators are more efficient in describing some situations since they capture non-localities and have memory effects [41]. Fractional operators have been used to model many real problems, such as photo acoustic [42, 43], viscoelastic properties [44], Quantum Mechanics [45–47], Epidemiology [48, 49], Ecology [50, 51], Duffing oscillator [52] and many others [53–55].

The dynamical behavior of the cancer model proposed by Itik and Banks [30] was studied in light of fractional operators in Ref. [56]. It was considered three different fractional derivatives formulations: the power-law [57] (singular kernel), the exponential [58], and the Mittag-Leffler [59]. The results show that the dynamics is changed as a consequence of the extension to fractional differential operators. Ghanbari [60] also explored the same model and investigated the influence of power-law, exponential decay-law, and Mittag-Leffler in the fractal-fractional approach. These researchers obtained conditions for the existence and uniqueness of the solutions and expanded a numerical method to study the dynamical behavior. The results showed that the dynamics change from chaotic to a limit cycle depending on the fractional order. Naik *et al.* [61], considering an extension given by the Caputo derivative, analyzed the stability of the model. In a numerical scheme, they reported that the system goes to a limit cycle in a chaotic regime for the standard model. Xuan *et al.* [62], using the Caputo fractal-fractional derivative in the cancer model, demonstrated that hidden attractors emerge under fractional operators. To study the system's complexity, they studied bifurcation diagrams and stability. Their findings also showed that the system converges to a limit cycle attractor when the fractional order is decreased. These works extend the model of Itik and Banks [30]. Extensions of other cancer models can be found in Refs. [63–72].

In this work, we analyze the influence of fractional operators in a cancer model [30]. As a definition of the fractional operator, we follow the Caputo scheme [41], with an order equal to α . We consider the parameters in which the trajectories are chaotic [31]. As a novelty, we characterize the model using recurrence quantification, such as recurrence rate (RR), recurrence time entropy (RTE), and determinism (DET). Furthermore, we localize the α value in which the system transits from chaos to limit

cycle utilizing RTE. Also, considering the mean square deviation of the time series, we construct the plane parameters composed of $\rho_1 \times \alpha$, where ρ_1 is the tumor growth. Our results suggest an exponential relation between α and tumor growth rate ρ_1 in which the dynamics transit from the limit cycle to a fixed point. This transition depends on a super transient time that follows the same relationship between ρ_1 and α .

Our work is organized as follows. In Section 2, we revisit the integer-order model analyzing the fixed points and their stabilities. Section 3 discusses the fractional influences in the cancer model. Our conclusions are drawn in Section 4.

2 Standard model

We consider a cancer model that describes the interactions among host cells (H), effector immune cells (E) and tumor cells (T), governed by the following equations:

$$\frac{dH}{dt} = \rho_1 H \left(1 - \frac{H}{\kappa_1}\right) - \alpha_{13} TH, \quad (1)$$

$$\frac{dE}{dt} = \rho_2 \frac{TE}{T + \kappa_2} - \alpha_{23} TE - \delta_2 E, \quad (2)$$

$$\frac{dT}{dt} = \rho_3 T \left(1 - \frac{T}{\kappa_3}\right) - \alpha_{31} TH - \alpha_{32} TE. \quad (3)$$

Equation 1 describes the growth of the host cells by a logistic function with a rate equal to ρ_1 and biotic capacity equal to κ_1 . The host cells are killed by tumor cells. This term is represented by the interaction $-\alpha_{13} TH$, where α_{13} is the host cell killing rate by tumor cells. Equation 2 gives the rate at which immune cells appear. These cells are the tumor antigens whose growth depends on the quantity of T , the growth rate of effector immune cells (ρ_2), and a positive constant κ_2 . The tumor cell not only contributes to the growth of immune cells but also to its death. In the term $-\alpha_{23} TE$, α_{23} is the rate at which tumor cells inhibit the immune cells. In addition, the E cells die according to δ_2 . The last equation, Eq. 3, gives the dynamics of the tumor cells. Similarly, with the H cells, the tumor growth is given by a logistic function with a growth rate equal to ρ_3 and biotic capacity equal to κ_3 . The T cells are killed by H cells at a rate equal to α_{31} and by the E cells with a rate equal to α_{32} .

Considering the transformation $(H, E, T) \rightarrow (x, y, z)$ [30], the normalized equations are

$$\frac{dx}{dt} = \rho_1 x(1 - x) - \alpha_{13} xz, \quad (4)$$

$$\frac{dy}{dt} = \frac{\rho_2 yz}{1 + z} - \alpha_{23} yz - \delta_2 y, \quad (5)$$

$$\frac{dz}{dt} = z(1 - z) - xz - \alpha_{32} yz. \quad (6)$$

A schematic representation of the model is displayed in Fig. 1. The red, green, and blue circles represent the x , y , and z cells, respectively. The arrows indicate the interactions. If the interaction is constructive (growth cells), we denote with a signal $+$. If the

interaction is destructive (kill cells), we denote it by a signal $-$. The x cells growth with a rate ρ_1 , which is indicated by $+\rho_1$ in Fig. 1. The x cells are killed by the tumor cells at a rate equal to α_{13} . The tumor cells grow according to a rate ρ_3 and are killed by x cells at a rate α_{31} and by y at a rate equal to α_{32} . The y cells grow when interacting with tumor cells by a rate ρ_2 and are killed by z cells according to a rate equal to α_{23} . Also, the y cells have a natural death δ_2 . The immune cells do not interact with the host cells. In this way, the tumor cells are the generalist competitors and the other two are specialist competitors [31]. In this type of interaction, there is no particular prey.

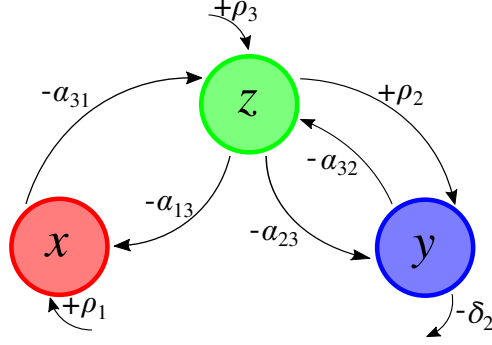


Fig. 1 Schematic representation of the cancer model. x , y and z represent the host, immune, and tumor cells. ρ_1 is the growth rate of x , α_{13} is the death rate of x due to z , α_{31} is the death rate of z due to x , ρ_3 is the growth rate of z , α_{32} is the death rate of z due to y , ρ_2 is the growth rate of y due to z , α_{23} is the death rate of y due to z and δ_2 is the natural death of y .

The fixed point solutions of this model are found by solving:

$$0 = \rho_1 x(1 - x) - \alpha_{13} x z, \quad (7)$$

$$0 = \frac{\rho_2 y z}{1 + z} - \alpha_{23} y z - \delta_2 y, \quad (8)$$

$$0 = z(1 - z) - x z - \alpha_{32} y z, \quad (9)$$

admitting seven solutions, that are $F_i \equiv (x^i, y^i, z^i)$, where $i = 1, \dots, 7$. Solving Eqs. 7, 8 and 9, we obtain

$$F_1 = (0, 0, 0), \quad F_2 = (0, 0, 1), \quad F_3 = (1, 0, 0) \quad (10)$$

$$F_4 = \left(0, \frac{\sqrt{(\alpha_{23} + \delta_2 - \rho_2)^2 - 4\alpha_{23}\delta_2} + 3\alpha_{23} + \delta_2 - \rho_2}{2\alpha_{23}\alpha_{32}}, \right. \\ \left. - \frac{\sqrt{(\alpha_{23} + \delta_2 - \rho_2)^2 - 4\alpha_{23}\delta_2} + \alpha_{23} + \delta_2 - \rho_2}{2\alpha_{23}} \right) \quad (11)$$

$$F_5 = \left(\frac{\alpha_{13} \left(\sqrt{-2\rho_2(\alpha_{23} + \delta_2) + (\alpha_{23} - \delta_2)^2 + \rho_2^2} + \alpha_{23} + \delta_2 - \rho_2 \right)}{2\alpha_{23}\rho_1} + 1, \right.$$

$$\begin{aligned}
& - \frac{(\alpha_{13} - \rho_1) \left(\sqrt{(\alpha_{23} + \delta_2 - \rho_2)^2 - 4\alpha_{23}\delta_2} + \alpha_{23} + \delta_2 - \rho_2 \right)}{2\alpha_{23}\alpha_{32}\rho_1}, \\
& - \frac{\sqrt{(\alpha_{23} + \delta_2 - \rho_2)^2 - 4\alpha_{23}\delta_2} + \alpha_{23} + \delta_2 - \rho_2}{2\alpha_{23}}, \tag{12}
\end{aligned}$$

$$\begin{aligned}
F_6 = & \left(0, -\frac{\sqrt{(\alpha_{23} + \delta_2 - \rho_2)^2 - 4\alpha_{23}\delta_2} - 3\alpha_{23} - \delta_2 + \rho_2}{2\alpha_{23}\alpha_{32}}, \right. \\
& \left. \frac{\sqrt{(\alpha_{23} + \delta_2 - \rho_2)^2 - 4\alpha_{23}\delta_2} - \alpha_{23} - \delta_2 + \rho_2}{2\alpha_{23}} \right), \tag{13}
\end{aligned}$$

$$\begin{aligned}
F_7 = & \left(\frac{\alpha_{13} \left(-\sqrt{-2\rho_2(\alpha_{23} + \delta_2)} + (\alpha_{23} - \delta_2)^2 + \rho_2^2 + \alpha_{23} + \delta_2 - \rho_2 \right)}{2\alpha_{23}\rho_1} + 1, \right. \\
& \frac{(\alpha_{13} - \rho_1) \left(\sqrt{(\alpha_{23} + \delta_2 - \rho_2)^2 - 4\alpha_{23}\delta_2} - \alpha_{23} - \delta_2 + \rho_2 \right)}{2\alpha_{23}\alpha_{32}\rho_1}, \\
& \left. \frac{\sqrt{(\alpha_{23} + \delta_2 - \rho_2)^2 - 4\alpha_{23}\delta_2} - \alpha_{23} - \delta_2 + \rho_2}{2\alpha_{23}} \right). \tag{14}
\end{aligned}$$

To simplify the analysis of the fixed points, the parameters are equal to $\alpha_{13} = 1.5$, $\rho_2 = 4.5$, $\alpha_{23} = 0.2$, $\delta_2 = 0.5$ and $\alpha_{32} = 2.5$. ρ_1 is maintained as our control parameter in the entire work. For these values, the fixed points are $F_1 = (0, 0, 0)$, $F_2 = (0, 0, 1)$, $F_3 = (1, 0, 0)$, $F_4 = (0, 0.3469, 0.1325)$, $F_5 = \frac{1}{\rho_1}(\rho_1 - 0.1987, 0.0530(1.5 - \rho_1), 0.1325\rho_1)$, $F_6 = (0, -7.1470, 18.8675)$ and $F_7 = \frac{1}{\rho_1}(\rho_1 - 28.3012, 7.5470(1.5 - \rho_1), 18.8675\rho_1)$. F_1 is a trivial solution and exhibits a population without cells. The eigenvalues associated with the Jacobian calculated in F_1 are $(1, -0.5, \rho_1)$. The signs depend on ρ_1 , which is always positive. Then, we find two unstable and one stable point, which characterize a saddle. F_2 is the point that represents a situation where the cancer cells occupy the whole host. The Jacobian eigenvalues in F_2 are $(1.55, \rho_1 - 1.5, -1)$. Considering $\rho_1 = 0.6$, we obtain $(1.55, -0.9, -1)$, which characterizes a saddle point. F_3 corresponds to the cancer-free solution. The Jacobian eigenvalues calculated at this point are $(0, -0.5, -\rho_1)$, as $\rho_1 \geq 0$, we have two negative eigenvalues and one equal zero. Thus, this point is a saddle. In F_4 , all coordinates are positives; all solutions are in the positive octant. The Jacobian eigenvalues in this point are $(\rho_1 - 0.198754, -0.0662515 + 0.6131239i, -0.0662515 - 0.6131239i)$. The F_5 point has a biological significance for $\rho_1 \in [0.1987, 1.5]$. Selecting $\rho_1 = 0.6$, we obtain $(0.6688, 0.0795, 0.1325)$ which is an unstable point. The F_6 point has a negative term associated with the effector immune cells. Therefore, this solution does not have biological relevance. F_7 has a biological relevance when $\rho_1 \geq 28.3012$. However, considering this range, the second element of F_7 is negative. This way, the point F_7 is irrelevant.

The numerical solutions for Eqs. 4 (blue line), 5 (red line) and 6 (green line) are displayed in Fig. 2(a) for $\rho_1 = 0.4$, $\alpha_{13} = 1.5$, $\rho_2 = 4.5$, $\alpha_{23} = 0.2$, $\alpha_{32} = 2.5$ and $\delta_2 = 0.5$. For these parameters, the solution is a limit cycle. The solutions show that

the number of host cells decreases while the immune and cancer increase. After that, the solution reaches an oscillatory behavior between the three population cells. For different ρ_1 values, it is possible to observe chaotic solutions. As shown in previous works [31], the dynamical system has a chaotic attractor for $\rho_1 = 0.6$, as exhibited in Fig. 2(b). Fig. 2(c) shows the 2-dimensional projection together with the fixed points.

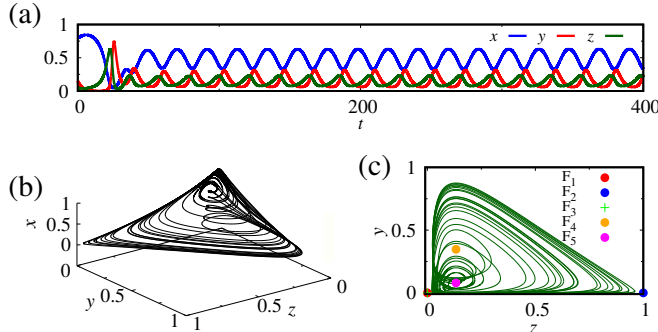


Fig. 2 (a) Time series for x , y and z in blue, red and green lines, respectively. In panel (a), we consider $\rho_1 = 0.4$. (b) Phase space in 3-dimensional space and projection in the plane $y - z$ in the panel (c) for $\rho_1 = 0.6$. We consider $\alpha_{13} = 1.5$, $\rho_2 = 4.5$, $\alpha_{23} = 0.2$, $\delta_2 = 0.5$, $\alpha_{32} = 2.5$, $x_0 = 0.80$, $y_0 = 0.15$, and $z_0 = 0.05$.

In order to distinguish periodic dynamics from chaotic ones, we use the recurrence plots (RPs), namely, recurrence quantification analysis (RQA), which remain valid under fractional operators. The RPs, introduced by Eckmann *et al.* [73], provide a visual representation of recurrences of the states of a system in a d -dimensional phase space within a small deviation ϵ , as well as a quantitative analysis of the dynamical behavior exhibited by the system. For this purpose, given a trajectory $\vec{x}(t) \in \mathbb{R}^d$, we define a recurrence matrix \mathbf{R} as

$$R_{ij} = H(\epsilon - \|\vec{x}(t_i) - \vec{x}(t_j)\|), \quad (15)$$

where $i, j = 1, 2, \dots, N$, N is the length of the time series, H is the Heaviside unit step function, ϵ is a small threshold and $\|\vec{x}(t_i) - \vec{x}(t_j)\|$ is the spatial distance between two states, $\vec{x}(t_i)$ and $\vec{x}(t_j)$, in phase space in terms of a suitable norm.

The recurrence matrix is symmetric and binary with the elements 0 representing the non-recurrent states and the elements 1 representing the recurrent ones. Two states are recurrent when the state at $t = t_i$ is close (up to a distance ϵ) to a different state at $t = t_j$. For the threshold ϵ , we choose it to be $\epsilon = 0.01$. For a discussion on the choice of ϵ , see Appendix.

Several measures based on the RPs have been proposed [74–78]. The most simple of them is the recurrence rate, RR, defined as

$$\text{RR} = \frac{1}{N^2} \sum_{i,j=1}^N R_{ij}, \quad (16)$$

which is a measure of the density of recurrent points. There are also measures based on the diagonal lines formed in an RP, such as determinism (or predictability)

$$\text{DET} = \frac{\sum_{\ell=\ell_{\min}}^N \ell P(\ell)}{\sum_{\ell=1}^N \ell P(\ell)}, \quad (17)$$

where $P(\ell)$ is the total number of diagonal lines with length ℓ and minimal length ℓ_{\min} . Determinism is also a density as the recurrence rate. It is the density of recurrent points that lie on a diagonal line and refers to the degree to which the dynamics of a system is predictable and repeatable over time. Systems with stochastic or chaotic behaviors cause no or very short diagonal lines, whereas deterministic behavior exhibits longer diagonal lines. Therefore, the determinism is expected to be small in the first case and large in the second case. There are also measures based on the vertical lines of length v , such as the laminarity (LAM) and the trapping time (TT), for example. For a detailed discussion about these and other measures, see Refs. [74–78] and references therein.

Entropy-based measures of RPs have been employed to characterize the dynamical behavior of nonlinear systems [79–84, 89]. The entropy of the distribution of recurrence times (recurrence time entropy) has been utilized as a tool for the detection of chaotic orbits. The vertical distances between the diagonal lines, *i.e.*, the gaps between them, are an estimate of the recurrence times of the trajectory [85–88]. The Shannon entropy of the distribution of white vertical lines (the estimate of the recurrence times) is defined as [79, 84, 89]

$$\text{RTE} = - \sum_{v=v_{\min}}^{v=v_{\max}} p_w(v) \ln p_w(v), \quad (18)$$

where v_{\min} (v_{\max}) is the length of the shortest (longest) white vertical line. $p_w(v) = P_w(v)/N_w$ and $P_w(v)$ are the relative distribution and the total number of white vertical lines of length v , respectively, and N_w is the total number of them. Due to the finite size of a RP, the distribution of white vertical lines might be biased by the white border lines, which are cut short by the border of the RP, thus affecting the RQA measures, such as the RTE [90]. In order to avoid these border effects, it is necessary to exclude the distribution of the lines that begin and end at the border of the RP.

To investigate the dynamic behavior of the cancer model, we consider ρ_1 as the control parameter and compute the bifurcation diagram by recording the local maxima, x_{\max} (black dots) and local minima, x_{\min} (red dots), of $x(t)$, as shown in Fig. 3(a). For $\rho_1 < 0.5$, the dynamics is periodic and becomes chaotic via period doubling. The bifurcation diagram exhibits some periodic windows. We consider the Lyapunov exponents (λ) as a classical method to compute chaotic solutions. Figure 3(b) shows the largest, λ_1 and second largest, λ_2 , Lyapunov exponents by the blue and red lines, respectively. The chaotic regimes are marked by at least one Lyapunov exponent greater than zero. In the periodic windows, we observe $\lambda_1 \approx 0$ and $\lambda_2 < 0$. On the other hand, when the dynamics is chaotic, $\lambda_1 > 0$. We also calculate the RQA measures RR, DET, and RTE in panels (c), (d), and (e), respectively. To construct the recurrence matrix, we consider the time series of x_{\max} , $\{x_{\max}^{(i)}\}_{i=1,2,\dots,N}$. We verify that periodic solutions exhibit large values of RR and DET, with $\text{DET} \rightarrow 1$, indicating that all recurrent

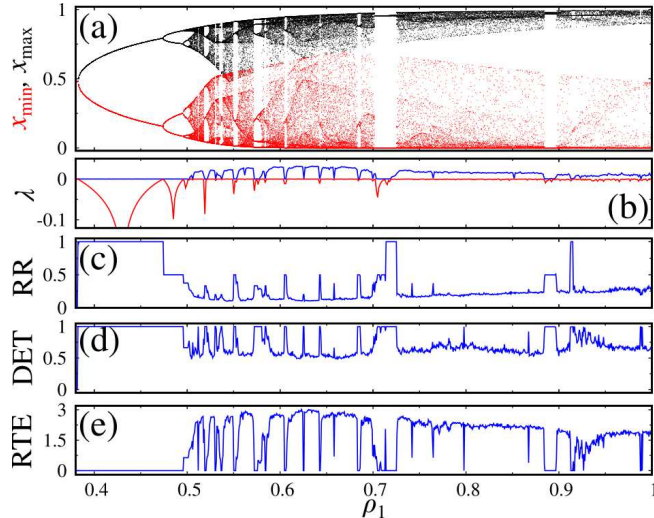


Fig. 3 (a) Bifurcation diagram of x_{\max} (black points) and x_{\min} (red points), (b) largest (blue line) and second largest Lyapunov (red line) exponents, (c) recurrence rate, RR, (d) determinism, DET, and (e) recurrence time entropy, RTE, as a function of ρ_1 . We consider $\alpha_{13} = 1.5$, $\rho_2 = 4.5$, $\alpha_{23} = 0.2$, $\delta_2 = 0.5$, $\alpha_{32} = 2.5$, and $\epsilon = 0.01$.

points lie on a diagonal line, whereas the RTE is close to zero in these cases. RR and DET show smaller values during the chaotic windows, while the RTE is larger. Therefore, there is a correlation between λ_1 and these RQAs measures. To quantify this correlation, we use the Pearson correlation coefficient,

$$\rho_{x,y} = \frac{\text{cov}(x,y)}{\sigma_x \sigma_y}, \quad (19)$$

where $\text{cov}(x,y)$ is the covariance between the two data series and σ their respective standard deviation. We obtain for the correlation coefficient between λ_1 and RR, DET, and RTE, the values $\rho_{\lambda_1, \text{RR}} = -0.54$, $\rho_{\lambda_1, \text{DET}} = -0.41$, $\rho_{\lambda_1, \text{RTE}} = 0.88$, respectively. Thus, the RTE is a great alternative for the characterization of the dynamics of this system.

3 Fractional approach

The fractional extension of the model described by Eqs. (4), (5) and (6) is obtained by making the following substitution: $Df \rightarrow D^\alpha f$, where D is the integer differential operator, i.e., df/dt and ${}_0D_t^\alpha f$ is the fractional differential operator and is defined, in the Caputo sense, by

$${}_0D_t^\alpha f \equiv \frac{1}{\Gamma(1-\alpha)} \int_0^t dt' \frac{1}{(t-t')^\alpha} \frac{\partial}{\partial t'} f(\vec{r}, t'), \quad (20)$$

where $\Gamma(\cdot)$ is the gamma function and $0 < \alpha < 1$ [41]. Therefore, the extended cancer model is given by

$${}_0D_t^\alpha x = \rho_1 x(1-x) - \alpha_{13} xz, \quad (21)$$

$${}_0D_t^\alpha y = \frac{\rho_2 yz}{1+z} - \alpha_{23} yz - \delta_2 y, \quad (22)$$

$${}_0D_t^\alpha z = z(1-z) - xz - \alpha_{32} yz. \quad (23)$$

The time series for $\alpha = 0.995$ (blue line), $\alpha = 0.98$ (red line) and $\alpha = 0.95$ (green line) are displayed in Fig. 4. The numerical integration is made by the algorithm described in Ref. [95]. The black dotted lines are for the standard case, as exhibited in Fig. 2. These results show that the fractional order attenuates the oscillations until a fixed point as α decreases. For instance, for $\alpha = 0.95$, the fixed point is equal to $(x, y, z) = (0.5032, 0.1456, 0.1325)$, which corresponds to F_5 calculated for $\rho_1 = 0.4$.

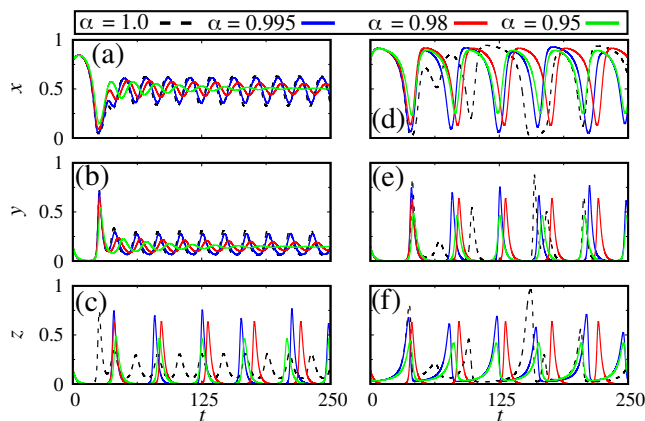


Fig. 4 Time series for x in the panels (a) and (d), for y in the panels (b) and (e), and for z in panels (c) and (f). The panels (a-c) are for $\rho_1 = 0.4$ and (d-f) for $\rho_1 = 0.6$. The black dotted lines are for $\alpha = 1.0$, the blue line is for $\alpha = 0.995$, the red line is for $\alpha = 0.98$ and the green line is for $\alpha = 0.95$. We consider $\alpha_{13} = 1.5$, $\rho_2 = 4.5$, $\alpha_{23} = 0.2$, $\delta_2 = 0.5$, $\alpha_{32} = 2.5$, $x_0 = 0.80$, $y_0 = 0.15$, and $z_0 = 0.05$.

The oscillatory behavior is attenuated in the chaotic regime for $\rho_1 = 0.6$ and the dynamics is transited to periodic behavior. By computing the RTE as a function of α , we see that there are some periodic windows. For $\alpha \gtrsim 0.9966$, the dynamics become periodic (Fig. 5(a)). The RTE information agrees with the bifurcation diagram, as shown in Fig. 5(b). The red and black points correspond to the x minimum and maximum values. The attractors in Fig. 6 display that the periodic behavior is a limit cycle that converges to a fixed point as α approaches to 0.9. The green line is for $\alpha = 0.995$, the red line for $\alpha = 0.975$, the blue line for $\alpha = 0.936$, the orange line for $\alpha = 0.915$ and the black dotted point for $\alpha = 0.885$.

One way to differentiate fixed points and limit cycles is by computing the mean standard deviation (σ). To do that, we discard a transient time (τ). Considering this time series, we compute σ . Figure 7(a) displays the parameter plane $\rho_1 \times \alpha$ as a

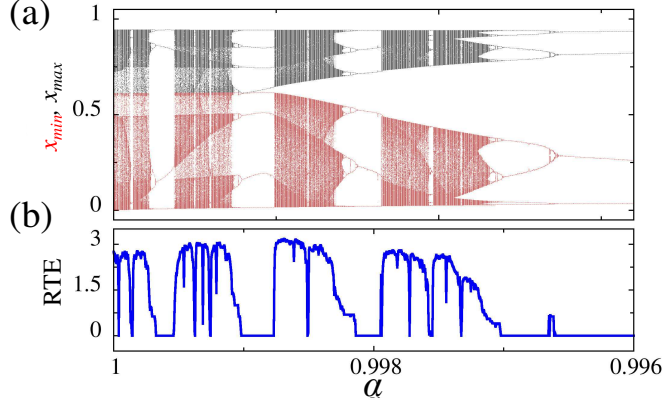


Fig. 5 (a) RTE and (b) bifurcation diagram as a function of α . We consider $\alpha_{13} = 1.5$, $\rho_1 = 0.6$, $\rho_2 = 4.5$, $\alpha_{23} = 0.2$, $\delta_2 = 0.5$, $\alpha_{32} = 2.5$, $x_0 = 0.80$, $y_0 = 0.15$, $z_0 = 0.05$, and $\epsilon = 0.01$.

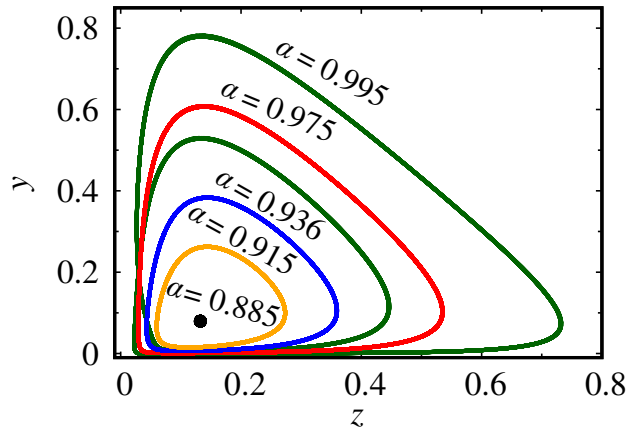


Fig. 6 Phase portrait for different α values. The green curve is for $\alpha = 0.995$, the red curve for $\alpha = 0.975$, the blue curve for $\alpha = 0.936$, the orange curve for $\alpha = 0.915$ and the black dot for $\alpha = 0.885$. We consider $\rho_1 = 0.6$, $\alpha_{13} = 1.5$, $\rho_2 = 4.5$, $\alpha_{23} = 0.2$, $\delta_2 = 0.5$, and $\alpha_{32} = 2.5$.

function of σ in color scale. The black points indicate when the solution is a fixed point ($\sigma < 10^{-3}$) and the colorful points indicate limit cycle solutions. Although some black points are mixed with colorful ones, a relation between α and ρ_1 separates most parts of the limit cycle from the fixed point solutions. This curve is indicated by the white dotted line in the panel (a) and is given by $\alpha = \beta_1 e^{\beta_2 \rho_1} + \beta_3 e^{\beta_4 \rho_1}$, where $\beta_1 = 3.150$, $\beta_2 = -7.800$, $\beta_3 = 0.808$ and $\beta_4 = 0.110$. Figure 7(b) exhibits the same plane parameter with the time to the solution for one initial condition reaches the steady solution in the color scale. The black dotted line indicates a region of super transient, which is defined by $\alpha = \xi_1 e^{\xi_2 \rho_1} + \xi_3 e^{\xi_4 \rho_1}$, where $\xi_1 = 3.25$, $\xi_2 = -7.7$, $\xi_3 = 0.802$, and $\xi_4 = 0.108$. Note that $\beta_i \approx \xi_i$. In this way, the transition from the limit cycle to fixed points crosses a super transient region.

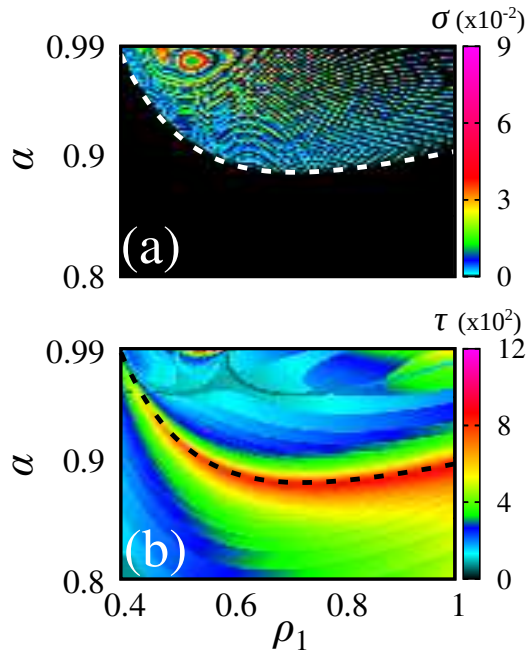


Fig. 7 $\rho_1 \times \alpha$ as a function of σ (mean standard deviation) in the panel (a) and τ (average transient time) in the panel (b). We consider $\alpha_{13} = 1.5$, $\rho_2 = 4.5$, $\alpha_{23} = 0.2$, $\delta_2 = 0.5$, and $\alpha_{32} = 2.5$.

As our results suggest, the transition from a limit cycle to fixed points is associated with a super transient time. In this way, we select $\rho_1 = 0.6$ and compute the mean transient time $\langle \tau \rangle$ for 100 different initial conditions close to the critical point. The critical point defines the transition and equals $\alpha_c = 0.899$. Figure 8 shows the mean transient time ($\langle \tau \rangle$) as a function of $|\alpha - \alpha_c|$ by the black points. The average transient lifetime scales with α as a power-law according to

$$\langle \tau \rangle \propto |\alpha - \alpha_c|^\gamma, \quad (24)$$

and has two slopes. By fitting the data (red line in Fig. 8), we obtain an exponent of $\gamma \approx -3/2$, with a correlation coefficient of 0.98 and $\gamma \approx -1/3$ (green line) with a correlation coefficient of 0.99. All the points evolve to F_5 .

4 Conclusions

In this work, we consider a fractional extension of a cancer model. This model describes the interactions among host, effector immune, and tumor cells. Due to the non-linearity, the dynamical behavior exhibits chaotic solutions for some parameter ranges. For the equations that govern the model, we obtain analytical solutions for the fixed points and discuss their stability.

In order to study a more broad case, we consider numerical solutions. As previously reported works, we verify chaotic solutions for $\rho_1 = 0.6$. Furthermore, we

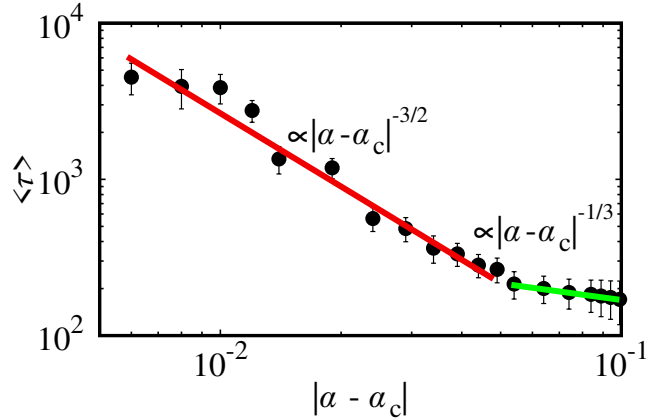


Fig. 8 $\langle \tau \rangle$ versus $|\alpha - \alpha_c|$, where $\alpha_c = 0.899$. The curve has two slopes, in the red curve $\gamma \approx -3/2$ and in the green $\gamma \approx -1/3$. The respective correlation coefficients are 0.98 and 0.99. We consider $\rho_1 = 0.6$, $\alpha_{13} = 1.5$, $\rho_2 = 4.5$, $\alpha_{23} = 0.2$, $\delta_2 = 0.5$, and $\alpha_{32} = 2.5$.

construct bifurcation diagrams considering the maxima and minimum points of the host cells. The dynamical behavior exhibited by the bifurcation diagram also was verified by the Lyapunov exponents and recurrence quantification analysis (RQA) measures. With regard to the RQA measures, we compute the recurrence rate (RR), determinism (DET), and recurrence time entropy (RTE). All three of them agree with the results from the Lyapunov exponents. By computing the Pearson correlation coefficient between them and λ_1 , we observe a higher coefficient for the RTE. Thus, we consider only the RTE to analyze the effects of fractional order.

We study the effects of fractional operators in the cancer model by the Caputo definition. Our main goal is to understand what happens in the chaotic behavior. By computing the RTE, our results suggest that the dynamical system becomes periodic for $\alpha \gtrsim 0.9966$. When we look for the phase portrait, the results show that the solutions transit from a limit cycle to a fixed point, which is equal to the fixed points calculated analytically. The limit cycle regime is in the range $\alpha \in (0.9966, 0.899)$ for $\rho_1 = 0.6$. For different ρ_1 values, we construct the parameter space $\rho_1 \times \alpha$ as a function of the mean standard deviation σ . Values of σ close to zero show fixed point solutions. Our results show the existence of an exponential curve that delimits fixed point solutions from limit cycles in this parameter space. Also, we analyze the transient time related to the transition from the limit cycle to a fixed point. For $\rho_1 = 0.6$, we find that for $\alpha < 0.899$ the dynamics go to the fixed point F_5 by a super transient with order 10^4 . The super transient curve follows a linear decay according to two slopes, equal to $-3/2$ and $-1/3$.

Acknowledgments

This work was possible with partial financial support from the following Brazilian government agencies: CNPq, CAPES, Fundação Araucária and São Paulo Research Foundation (FAPESP 2018/03211-6, 2022/13761-9). R. L. V. received partial financial

support from the following Brazilian government agencies: CNPq (403120/2021-7, 301019/2019-3), CAPES (88881.143103/2017-01), FAPESP (2022/04251-7). E. K. L. received partial financial support from the following Brazilian government agency: CNPq (301715/2022-0). E.C.G. received partial financial support from Coordenação de Aperfeiçoamento de Pessoal de Nível Superior - Brasil (CAPES) - Finance Code 88881.846051/2023-01. We would like to thank the 105 Group Science (www.105groupscience.com).

Declarations

Conflict of Interest:

The author declares that there exists no competing financial interest or personal relationships that could have appeared to influence the work reported in this paper.

Appendix

In Section 2, we introduced the cancer model and analyzed its dynamics for different parameter values by means of a bifurcation diagram, the Lyapunov exponents, and three RQA measures: RR, DET, and RTE. We chose the threshold ϵ to be $\epsilon = 0.01$. Many researchers have addressed the problem of finding the best value of ϵ [91–94]. Here, we used the correlation coefficient, Eq. (19), to determine ϵ . We computed the RTE as a function of ρ_1 for different threshold values, ranging from 10^{-5} to 10^{-1} , and calculated the correlation coefficient between λ_1 and RTE (Fig. 9). Even if we choose a very small ϵ (10^{-5}) or a relatively large ϵ (10^{-1}), we still obtain a rather high correlation coefficient, with the highest value being around $\epsilon \approx 10^{-2}$, and hence our choice of ϵ . Furthermore, the fact that $\rho_{\lambda_1, RTE}$ does not change too much within this range of ϵ indicates that, in our case, the choice of ϵ is not as sensible as it would be in other cases. In fact, there is a wide range of values for ϵ in which the results are good.

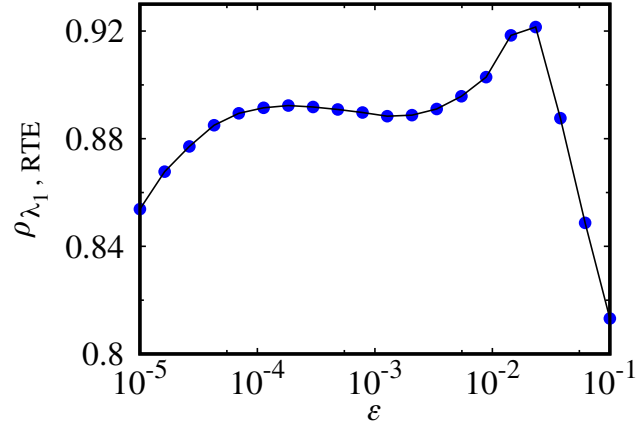


Fig. 9 The correlation coefficient between λ_1 and RTE as a function of the threshold ϵ .

References

- [1] Hausman DM. What is cancer? Perspectives in Biology and Medicine 2019;62(4):778-784.
- [2] Ferlay J, Colombet M, Soerjomataram I, Parkin DM, Piñeros M, Znaor A, Bray F. Cancer statistics for the year 2020: An overview. Cancer Epidemiology 2021;149:778-789.
- [3] Siegel RL, Miller KD, Fuchs HE, Jemal A. Cancer statistics, 2022. CA Cancer J Clin 2022;72:7-33.
- [4] Siegel RL, Miller KD, Jemal A. Cancer statistics, 2018. CA Cancer J Clin 2018;68:7-30.
- [5] Jones PA, Baylin SB. The Epigenomics of Cancer. Cell 2007;128:683-692.
- [6] Mufudza C, Sorofa W, Chiyaka ET. Assessing the Effects of Estrogen on the Dynamics of Breast Cancer. Computational and Mathematical Methods in Medicine 2012;473572.
- [7] Waldman AD, Fritz JM, Lenardo MJ. A guide to cancer immunotherapy: from T cell basic science to clinical practice. Nature Reviews Immunology 2020;20:651-668.
- [8] López AG, Seoane JM, Sanjuán MAF. Modelling Cancer Dynamics Using Cellular Automata. In: Berezovskaya, F., Toni, B. (eds) Advanced Mathematical Methods in Biosciences and Applications 2019;159-205.
- [9] Iarosz KC, Borges FS, Batista AM, Baptista MS, Siqueira RAN, Viana RL, Lopes SR. Mathematical model of brain tumour with glia–neuron interactions and chemotherapy treatment. Journal of Theoretical Biology 2015;368;113-121.
- [10] Trobia J, Gabrick EC, Seifert EG, Borges FS, Protachevicz PR, Szezech Jr. JD, Iarosz KC, Santos MS, Caldas IL, Tian K, Ren HP, Grebogi C, Batista AM. Effects of drug resistance in the tumour-immune system with chemotherapy treatment. Indian Academy of Sciences Conference Series 2020;3(1):39-44.
- [11] Trobia J, Tian K, Batista AM, Grebogi C, Pen HP, Santos MS, Protachevicz PR, Borges FS, Szezech Jr JD, Viana RL, Caldas IL, Iarosz KC. Mathematical model of brain tumour growth with drug resistance. Communications in Nonlinear Science and Numerical Simulation 2021;103:106013.
- [12] Castiglione F, Piccoli B. Cancer immunotherapy, mathematical modeling and optimal control. Journal of Theoretical Biology 2007;247(4):723-732.
- [13] López AG, Iarosz KC, Batista AM, Seoane JM, Viana RL, Sanjuán MAF. The role of dose density in combination cancer chemotherapy. Communications in

- [14] Borges FS, Iarosz KC, Ren HP, Batista AM, Baptista MS, Viana RL, Lopes SR, Grebogi C. Model for tumour growth with treatment by continuous and pulsed chemotherapy. *BioSystems* 2014;116:43-48.
- [15] Liu Z, Yang C. A Mathematical Model of Cancer Treatment by Radiotherapy. *Computational and Mathematical Methods in Medicine* 2014;2014:172923.
- [16] Mamat M, Subiyanto, Kartono A. Mathematical Model of Cancer Treatments Using Immunotherapy, Chemotherapy and Biochemotherapy. *Applied Mathematical Sciences* 2013;7(5):247-261.
- [17] Sayari E, da Silva ST, Iarosz KC, Viana RL, Szezech Jr JD, Batista AM. Prediction of fluctuations in a chaotic cancer model using machine learning. *Chaos, Solitons and Fractals* 2022;164:112616.
- [18] de Pillis LG, Radunskaya A. The Dynamics of an Optimally Controlled Tumor Model: A Case Study. *Mathematical and Computer Modelling* 2003;37:1221-1244.
- [19] Iarosz KC, Martins CC, Batista AM, Viana RL, Lopes SR, Caldas IL, Penna TJP. On a cellular automaton with time delay for modelling cancer tumors. *Journal of Physics: Conference Series* 2011;285:012015.
- [20] Kuznetsov VA, Makalkin IA, Taylor MA, Perelson AS. Nonlinear dynamics of immunogenic tumors: Parameter estimation and global bifurcation analysis. *Bulletin of Mathematical Biology* 1994;56(2):295-321.
- [21] Pinho STR, Freedman HI, Nani F. A chemotherapy model for the treatment of cancer with metastasis. *Mathematical and Computer Modelling: An International Journal* 2002;36(7-8):773-803.
- [22] Amatruda JF, Shepard JL, Stern HW, Zon LI. Zebrafish as a cancer model system. *Cancer Cell* 2002;1(3):229-231.
- [23] Altrock PM, Liu LL, Michor F. The mathematics of cancer: integrating quantitative models. *Nature Reviews Cancer* 2015;15:730-745.
- [24] Tuveson D, Clevers H. Cancer modeling meets human organoid technology. *Science* 2019;364(6444):952-955.
- [25] Dehingia K, Sarmah HK, Alharbi Y, Hosseini K. Mathematical analysis of a cancer model with time-delay in tumor-immune interaction and stimulation processes. *Advances in Difference Equations* 2021;2021:473.
- [26] Díaz-Marín H, López-Hernández JF, Osuna O. Stability and eradication of tumor in a model with almost periodically radiated cells. *Journal of Applied Mathematics and Computing* 2022;68:3781-3797.

- [27] López AG, Iarosz KC, Batista AM, Seoane JM, Viana RL, Sanjuán MAF. Nonlinear cancer chemotherapy: Modelling the Norton-Simon hypothesis. *Communications in Nonlinear Science and Numerical Simulation* 2019;70:307-317.
- [28] López AG, Seoane JM, Sanjuán MAF. A Validated Mathematical Model of Tumor Growth Including Tumor–Host Interaction, Cell-Mediated Immune Response and Chemotherapy. *Bulletin of Mathematical Biology* 2014;76:2884-2906.
- [29] Tél T, Gruiz M. *Chaotic dynamics: An introduction based on Classical Mechanics*. Cambridge University Press 2006.
- [30] Itik M, Banks SP. Chaos in a three-dimensional cancer model. *International Journal of Bifurcation and Chaos* 2010;20(1):71-79.
- [31] Letellier C, Denis F, Aguirre LA. What can be learned from a chaotic cancer model? *Journal of Theoretical Biology* 2013;322:7–16.
- [32] Khajanchi S, Perc M, Gosh D. The influence of time delay in a chaotic cancer model. *Chaos: An Interdisciplinary Journal of Nonlinear Science* 2018;28:103101.
- [33] Abernethy S, Gooding RJ. The importance of chaotic attractors in modelling tumour growth. *Physica A: Statistical Mechanics and its Applications* 2018;507:268-277.
- [34] Gallas MR, Gallas MR, Gallas JAC. Distribution of chaos and periodic spikes in a three-cell population model of cancer. *The European Physical Journal Special Topics* 2014;223:2131-2144.
- [35] Khajanchi S. Bifurcation analysis of a delayed mathematical model for tumor growth. *Chaos, Solitons and Fractals* 2015;77:264-276.
- [36] Kemwoue FF, Dongo JM, Mballa RN, Gninzanlong CL, Kemayou MW, Mokhtari B, Biya-Motto F, Atangana J. Bifurcation, multistability in the dynamics of tumor growth and electronic simulations by the use of Pspice. *Chaos, Solitons and Fractals* 2020;134:109689.
- [37] Li J, Xie X, Chen Y, Zhang D. Complex dynamics of a tumor-immune system with antigenicity. *Applied Mathematics and Computation* 2021;400:126052.
- [38] Valle PA, Coria LN, Gamboa D, Plata C. Bounding the Dynamics of a Chaotic-Cancer Mathematical Model. *Mathematical Problems in Engineering* 2018:9787015.
- [39] Uthamacumaran A. A review of dynamical systems approaches for the detection of chaotic attractors in cancer networks. *Patterns* 2021;2(4):100226.
- [40] Evangelista LR, Lenzi EK. *An Introduction to Anomalous Diffusion and Relaxation*, Springer Nature, 2023.

- [41] Evangelista LR, Lenzi EK. Fractional Diffusion Equations and Anomalous Diffusion, Cambridge University Press, 2018.
- [42] Somer A, Galovic S, Lenzi EK, Novatski A, Djordjevic K. Temperature profile and thermal piston component of photoacoustic response calculated by the fractional dual-phase-lag heat conduction theory. *International Journal of Heat and Mass Transfer* 2023;203:123801.
- [43] Somer A, Popovic MN, da Cruz GK, Novatski A, Lenzi EK, Galovic SP. Anomalous thermal diffusion in two-layer system: The temperature profile and photoacoustic signal for rear light incidence. *International Journal of Thermal Sciences* 2022;179:107661.
- [44] do Carmo WP, Santos AF, Lenzi MK, Fortuny M, Lenzi EK. A new fractional model applied to description of the viscoelastic creep behavior of two Brazilian oils and their w/o emulsions. *Digital Chemical Engineering* 2023;6:100069.
- [45] Cius D, Menon Jr L, dos Santos MAF, de Castro ASM, Andrade FM. Unitary evolution for a two-level quantum system in fractional-time scenario. *Physical Review E* 2022;106:054126.
- [46] Lenzi EK, Ribeiro HV, dos Santos MAF, Rossato R, Mendes RS. Time dependent solutions for a fractional Schrödinger equation with delta potentials. *Journal of Mathematical Physics* 2013;54(8):082107.
- [47] Gabrick EC, Sayari E, de Castro ASM, Trobia J, Batista AM, Lenzi EK. Fractional Schrödinger equation and time dependent potentials. *Communications in Nonlinear Science and Numerical Simulation* 2023;107275.
- [48] Srivastava HM, Saad KM, Khader MM. An efficient spectral collocation method for the dynamic simulation of the fractional epidemiological model of the Ebola virus. *Chaos, Solitons and Fractals* 2020;140:110174.
- [49] Dong NP, Long HV, Khastan A. Optimal control of a fractional order model for granular SEIR epidemic with uncertainty. *Communications in Nonlinear Science and Numerical Simulation* 2020;88:105312.
- [50] Kumar A, Kumar S. A study on eco-epidemiological model with fractional operators. *Chaos, Solitons and Fractals* 2022;156:111697.
- [51] Mahmoud EE, Trikha P, Jahanzaib LS, Almaghrabi OA. Dynamical analysis and chaos control of the fractional chaotic ecological model. *Chaos, Solitons and Fractals* 2020;141:110348.
- [52] Coccolo M, Seoane JM, Lenci S, Sanjuán MAF. Fractional damping effects on the transient dynamics of the Duffing oscillator. *Communications in Nonlinear Science and Numerical Simulation* 2023;117:106959.

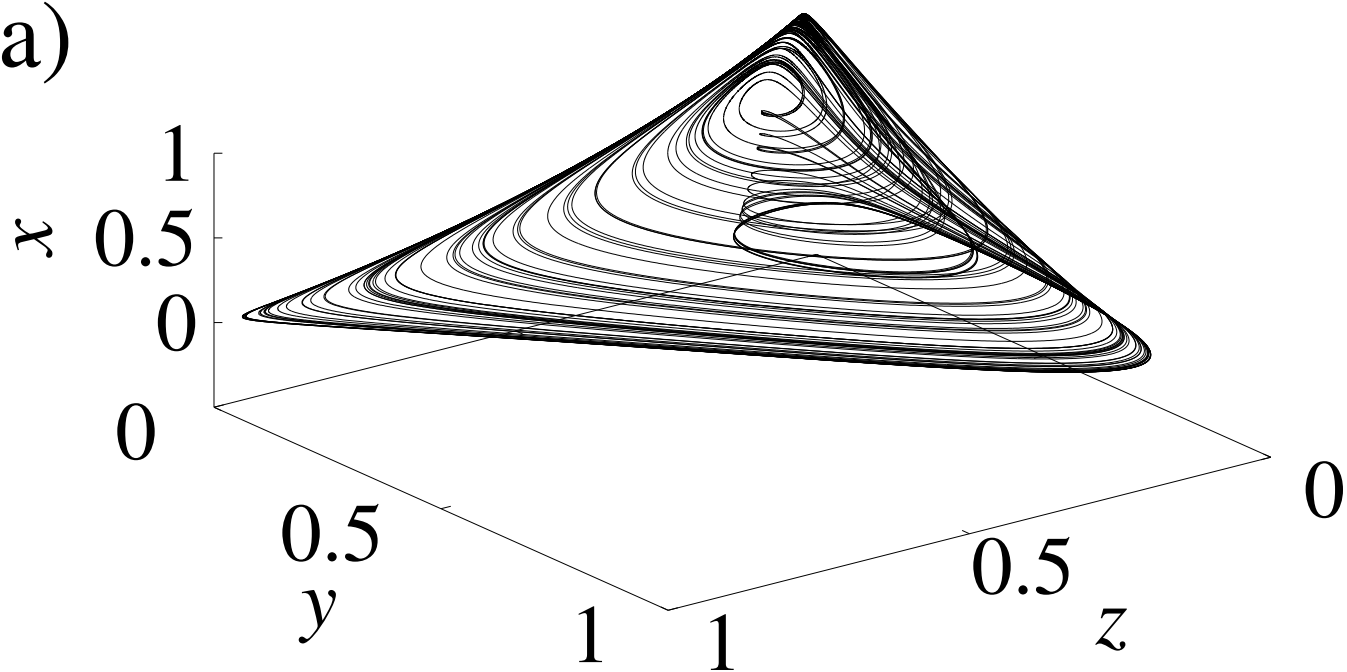
- [53] Nadeem M, Jafari H, Akgül A, De la Sen M. A Computational Scheme for the Numerical Results of Time-Fractional Degasperis–Procesi and Camassa–Holm Models. *Symmetry* 2022;14(12);2532.
- [54] Vivekanandhan G, Abdolmohammadi HR, Natiq H, Rajagopal K, Jafari S, Namazi H. Dynamic analysis of the discrete fractional-order Rulkov neuron map. *Mathematical Biosciences and Engineering* 2023;20(3);4760-4781.
- [55] Sun HG, Zhang Y, Baleanu D, Chen W, Chen Y. A new collection of real world applications of fractional calculus in science and engineering. *Communications in Nonlinear Science and Numerical Simulation* 2018;64;213-231.
- [56] Atangana A, Jain S. The role of power decay, exponential decay and Mittag-Leffler function's waiting time distribution: Application of cancer spread. *Physica A* 2018;512:330-351.
- [57] Caputo M, Fabrizio M. On the Singular Kernels for Fractional Derivatives. Some Applications to Partial Differential Equations. *Progress in Fractional Differentiation and Application* 2021;7(2):79-82.
- [58] Caputo M, Fabrizio M. A new Definition of Fractional Derivative without Singular Kernel. *Progress in Fractional Differentiation and Applications* 2015;1(2):73-85.
- [59] Atangana A, Baleanu D. New fractional derivatives with non-local and non-singular kernel: Theory and application to heat transfer model. *Thermal Science* 2016;20(2):763-769.
- [60] Ghanbari B. On the modeling of the interaction between tumor growth and the immune system using some new fractional and fractional-fractal operators. *Advances in Difference Equations* 2020;2020:585.
- [61] Naik PA, Zu J, Naik M. Stability analysis of a fractional-order cancer model with chaotic dynamics. *International Journal of Biomathematics* 2021;14(6):2150046.
- [62] Xuan L, Ahmad S, Ullah A, Saifullah S, Akgül A, Qu H. Bifurcations, stability analysis and complex dynamics of Caputo fractal-fractional cancer model. *Chaos, Solitons and Fractals* 2022;159:112113.
- [63] Ahmad S, Ullah A, Abdeljawad T, Akgül A, Mlaiki N. Analysis of fractal-fractional model of tumor-immune interaction. *Results in Physics* 2021;25:104178.
- [64] Ahmed E, Hashis AH, Riham FA. On fractional order cancer model. *Journal of Fractional Calculus and Applications* 2012;3(2):1-6.
- [65] Arfan M, Shah K, Ullah A, Shutaywi M, Kumam P, Shah Z. On fractional order model of tumor dynamics with drug interventions under nonlocal fractional derivative. *Results in Physics* 2021;21:103783.

- [66] Baleanu D, Jajarmi A, Sajjadi SS, Mozyrska D. A new fractional model and optimal control of a tumor-immune surveillance with non-singular derivative operator. *Chaos* 2019;29:083127.
- [67] Debbouche N, Ouannas A, Grassi G, Al-Hussein ABA, Tahir FR, Saad KM, Jahanshahi H, Aly AA. Chaos in Cancer Tumor Growth Model with Commensurate and Incommensurate Fractional-Order Derivatives. *Computational and Mathematical Methods in Medicine* 2022;5227503.
- [68] Hassani H, Machado JAT, Avazzadeh Z, Safari E, Mehrabi S. Optimal solution of the fractional order breast cancer competition model. *Scientific Reports* 2021;11:15622.
- [69] Iyiola OS, Zaman FD. A fractional diffusion equation model for cancer tumor. *AIP Advances* 2014;4:107121.
- [70] Kumar S, Ajay Kumar, Samet B, Gómez-Aguilar JF, Osman MS. A chaos study of tumor and effector cells in fractional tumor-immune model for cancer treatment. *Chaos, Solitons and Fractals* 2020;141:110321.
- [71] Rehaman MAU, Ahmad J, Hassan A, Awrejcewicz J, Pawlowski W, Karamti H, Alharbi FM. The Dynamics of a Fractional-Order Mathematical Model of Cancer Tumor Disease. *Symmetry* 2022;14:1694.
- [72] Solís-Pérez JE, Gómez-Aguilar JF, Atangana A. A fractional mathematical model of breast cancer competition model. *Chaos, Solitons and Fractals* 2019;127:38-54.
- [73] Eckmann JP, Kamphorst SO, Ruelle D. Recurrence Plots of Dynamical Systems. *Europhysics Letters* 1987;4(9):973.
- [74] Marwan N, Wessel N, Meyerfeldt U, Schirdewan A, Kurths J. Recurrence-plot-based measures of complexity and their application to heart-rate-variability data. *Phys. Rev. E* 2002;66(2):026702.
- [75] Marwan N, Kurths. Nonlinear analysis of bivariate data with cross recurrence plots. *Physics Letters A* 2002;302(5):299-307.
- [76] Marwan N. A historical review of recurrence plots. *The European Physical Journal Special Topics* 2008;164(1):3-12.
- [77] Bedartha G. A Brief Introduction to Nonlinear Time Series Analysis and Recurrence Plots. *Vibration* 2019;2(4):332-368.
- [78] Marwan N, Webber CL. *Mathematical and Computational Foundations of Recurrence Quantifications*. Springer International Publishing 2015.
- [79] Little MA, McSharry PE, Roberts SJ, Costello DAE, Moroz IM. Exploiting Non-linear Recurrence and Fractal Scaling Properties for Voice Disorder Detection.

- [80] Webber CL, Zbilut JP. Dynamical assessment of physiological systems and states using recurrence plot strategies. *Journal of Applied Physiology* 1994;76(2):965-973.
- [81] Trulla LL, Giuliani A, Zbilut JP, Webber CL. Recurrence quantification analysis of the logistic equation with transients. *Physics Letters A* 1996;223(4):255-260.
- [82] Ngamga EJ, Senthilkumar DV, Kurths J. Dynamics between order and chaos revisited. *The European Physical Journal Special Topics* 2010;191(1):15-27.
- [83] Eroglu D, Peron TKDM, Marwan N, Rodrigues FA, Costa LF, Sebek M, Kiss IZ, Kurths J. Entropy of weighted recurrence plots. *Physical Review E* 2014;90(4):042919.
- [84] Sales MR, Mugnaine M, Szezech Jr. D, Viana RL, Caldas IL, Marwan N, Kurths J. Stickiness and recurrence plots: An entropy-based approach. *Chaos: An Interdisciplinary Journal of Nonlinear Science* 2023;33(3):033140.
- [85] Zou Y, Thiel M, Romano MC, Kurths J. Characterization of stickiness by means of recurrence. *Chaos: An Interdisciplinary Journal of Nonlinear Science* 2007;17(4):
- [86] Zou Y, Pazó D, Romano MC, Thiel M, Kurths J. Distinguishing quasiperiodic dynamics from chaos in short-time series. *Phys. Rev. E* 2007;76(1):016210.
- [87] Baptista MS, Ngama EJ, Pinto PRF, Brito M, Kurths J. Kolmogorov–Sinai entropy from recurrence times. *Physics Letters A* 2010;374(9):1135-1140.
- [88] Ngamga EJ, Senthilkumar DV, Prasad A, Parmananda P, Marwan N, Kurths J. Distinguishing dynamics using recurrence-time statistics. *Phys. Rev. E* 2012;85(2):026217.
- [89] Kraemer KH, Donner RV, Heitzig J, Marwan N. Recurrence threshold selection for obtaining robust recurrence characteristics in different embedding dimensions. *Chaos: An Interdisciplinary Journal of Nonlinear Science* 2018;28(8):085720.
- [90] Kraemer KH, Marwan N. Border effect corrections for diagonal line based recurrence quantification analysis measures. *Physics Letters A* 2019;383(34):125977.
- [91] Zbilut JP, Zaldívar-Comenges JM, Strozzi F. Recurrence quantification based Liapunov exponents for monitoring divergence in experimental data. *Physics Letters A* 2002;297(3):173-181.
- [92] Thiel M, Romano MC, Kurths J, Meucci R, Allaria E, Arecchi FT. Influence of observational noise on the recurrence quantification analysis. *Physica D: Nonlinear Phenomena* 2002;171(3):138-152.

- [93] Schinkel S, Dimigen O, Marwan N. Selection of recurrence threshold for signal detection. *The European Physical Journal Special Topics* 2008;164(1):45-53.
- [94] Medrano J, Kheddar A, Annick L, Sofiane R. Radius selection using kernel density estimation for the computation of nonlinear measures. *Chaos: An Interdisciplinary Journal of Nonlinear Science* 2021;31(8):083131.
- [95] Garrappa R. Numerical Solution of Fractional Differential Equations: A Survey and a Software Tutorial. *Mathematics* 2018;6(16):1-23.

(a)



(b)

